Neuron, Vol. 33, 411–424, January 31, 2002, Copyright ©2002 by Cell Press

Differential Control of Vesicle Priming and Short-Term Plasticity by Munc13 Isoforms

Christian Rosenmund,[1,3] Albrecht Sigler,[1] Iris Augustin,[2] Kerstin Reim,[2] Nils Brose,[2] and Jeong-Seop Rhee[1]

[1] Max-Planck-Institut für Biophysikalische Chemie
Abteilung Membranbiophysik
Am Faßberg 11
D-37077 Göttingen
Bundesrepublik Deutschland

[2] Max-Planck-Institut für Experimentelle Medizin
Abteilung Neurogenetik
AG Molekulare Neurobiologie
Hermann-Rein-Str. 3
D-37075 Göttingen
Bundesrepublik Deutschland

Summary

Presynaptic short-term plasticity is an important adaptive mechanism regulating synaptic transmitter release at varying action potential frequencies. However, the underlying molecular mechanisms are unknown. We examined genetically defined and functionally unique axonal subpopulations of synapses in excitatory hippocampal neurons that utilize either Munc13-1 or Munc13-2 as synaptic vesicle priming factor. In contrast to Munc13-1-dependent synapses, Munc13-2-driven synapses show pronounced and transient augmentation of synaptic amplitudes following high-frequency stimulation. This augmentation is caused by a Ca^{2+}-dependent increase in release probability and releasable vesicle pool size, and requires phospholipase C activity. Thus, differential expression of Munc13 isoforms at individual synapses represents a general mechanism that controls short-term plasticity and contributes to the heterogeneity of synaptic information coding.

Introduction

Synapses in the central nervous system display a striking heterogeneity in presynaptic properties including morphology, release probability, and short-term plasticity (Harris and Stevens, 1989; Hessler et al., 1993; Rosenmund et al., 1993; Schikorski and Stevens, 1997; Walmsley et al., 1998). Interestingly, such heterogeneity is not only observed among synapses from different types of neurons, but is also detectable between synapses formed by a single axon of an individual nerve cell (Murthy et al., 1997; Reyes et al., 1998; Rosenmund et al., 1993; Scanziani et al., 1998; Thomson, 1997). In all of these cases, the molecular mechanisms underlying synapse heterogeneity are unknown, and its physiological relevance is unclear.

Presynaptic short-term plasticity allows a given synapse to rapidly alter its transmitter release characteristics in response to acute changes in activation patterns. Short-term plasticity is strongly dependent on the initial efficiency with which synapses transduce action potentials into synaptic transmitter release (Ma et al., 1999; Malgaroli, 1999; Rosenmund et al., 1993; Wadiche and Jahr, 2001). Synaptic responses of synapses with high initial release probability tend to depress even at low action potential frequencies because more synaptic vesicles from the pool of readily releasable vesicles are released than replenished. Synapses with low initial release probability, on the other hand, show initial facilitatory characteristics, but exhibit depression once the stimulation frequency is high enough. It is thought that neurons can increase vesicle recruitment rates in a use-dependent manner in order to maintain faithful information transfer during periods of increased release rates that approximate or exceed replenishment rates (Zucker, 1999). In almost all studies examining presynaptic short-term plasticity, alterations of presynaptic efficacy were associated with the buildup of intraterminal Ca^{2+} concentrations during high-frequency stimulation (Zucker, 1999). However, it is unclear, as to whether and by which mechanism Ca^{2+} triggers these short-term changes. Essentially, interference of Ca^{2+} with every step of the synaptic vesicle cycle could result in short-term changes of synaptic release probability. Thus, short-term plasticity may be caused by a direct effect of Ca^{2+} on proteins regulating vesicle translocation, tethering, docking, priming, fusion, or even endocytosis. In addition, rises in intraterminal Ca^{2+} concentrations could regulate cytoskeletal proteins or kinases/phosphatases which in turn modulate components of the synaptic release machinery.

Using deletion mutant (knockout) mice, we demonstrated recently that the presynaptic active zone component Munc13-1 is essential for synaptic vesicle priming in hippocampal neurons (Augustin et al., 1999b). Similar observations were made in knockout mutant *C. elegans* and *Drosophila* lacking the respective orthologs, Unc-13 or Dunc-13 (Aravamudan et al., 1999). One striking difference between the Munc13-1/Unc-13/Dunc-13 knockout mutant mouse and invertebrate phenotypes was that synaptic transmission was completely shutdown in mutant *C. elegans* and *Drosophila*, while in mice, the blocking effect of the mutation on vesicle priming was neurotransmitter specific and incomplete (Augustin et al., 1999b): GABAergic neurons were unaffected by Munc13-1 loss, and a subpopulation of synapses (10%) formed by individual glutamatergic Munc13-1 knockout neurons still produced fusion-competent vesicles and released glutamate with normal release probability. Indirect pharmacological evidence suggested that glutamatergic neurons form two types of synapses, one of which is completely Munc13-1 dependent while the other one uses an alternative vesicle priming protein. The most likely explanation for this phenomenon is redundancy between Munc13 isoforms. While the *C. elegans* and *Drosophila* contain only one *unc13/dunc13* gene each, the mammalian Munc13 family is comprised of three independent gene products (Munc13-1, Munc13-2, and Munc13-3; Augustin et al.,

[3] Correspondence: crosenm@gwdg.de

1999a), two of which (Munc13-1 and Munc13-2) are coexpressed in mouse hippocampus (Augustin et al., 1999a, 2001).

In the present study, we use Munc13-1 knockout, Munc13-2 knockout, and Munc13-1/2 double knockout mutant mice to determine the relative contribution of these two Munc13 isoforms to synaptic transmission in hippocampal neurons and to analyze their functional differences in determining short-term plasticity characteristics of synapses.

Results

We performed patch-clamp analyses on individual autaptic neurons (Bekkers and Stevens, 1991) from wild-type and Munc13-1 knockouts to study the characteristics of Munc13-1-dependent and Munc13-1-independent synapses. Excitatory glutamatergic and inhibitory GABAergic synaptic currents were distinguished by their pharmacological and kinetic properties.

Distinct Populations of Munc13-1-Dependent and Munc13-1-Independent Synapses in Individual Excitatory Neurons

Our previous work showed that glutamatergic Munc13-1 knockout neurons form normal numbers of synapses (Augustin et al., 1999b). These Munc13-1 knockout neurons were characterized by a 90% reduction in the readily releasable vesicle pool (RRP) and evoked transmitter release. Indirect assays to determine the fraction of active synapses in Munc13-1 knockouts indicated that the dramatic 90% deficit in transmitter release competence in Munc13-1 knockout was due to a complete shut down of the majority of glutamatergic Munc13-1 knockout synapses while the remaining 10% of synapses transmitted with normal release characteristics. To show this directly, we measured the fraction of active synapses in Munc13-1 knockout neurons by assaying the uptake and release of the fluorescent membrane dye FM1-43 with quantitative fluorescence microscopy (Cochilla et al., 1999).

Exocytotically active synapses were identified on fluorescence images from selected subregions of autaptic neurons by measuring the stimulation-induced decrease of FM1-43 fluorescence intensity (see Experimental Procedures). In each experiment, loading and unloading of FM1-43 in synaptic vesicles were performed twice, first with action potential trains (10–20 Hz; 10–15 s) and second with K^+-induced depolarization. Both data sets were analyzed independently and yielded similar activity patterns. The total synapse population was determined retrospectively by immunocytochemical staining for Synaptophysin and counting of synapses in the same regions that were examined in the FM1-43 experiments. Verifying our previous results, we found that the density of immunocytochemically defined Synaptophysin-positive synapses did not differ significantly between Munc13-1 knockout and wild-type cells (not shown). However, the fraction of active synapses, which is the ratio between the number of active synapses and the total Synaptophysin-positive synapse count, was 66.3% $\pm$ 18% for wild-type cells but only 9.4% $\pm$ 3.6% in Munc13-1 knockout neurons (Figures 1A–1D). This indicates that in excitatory/glutamatergic Munc13-1 knockout neurons, only a small subpopulation of synapses is active while the majority is presynaptically silent, and that the pool of active synapses in Munc13-1 knockout neurons employs another priming factor.

Munc13-1-Independent Synapses Employ Munc13-2 as a Priming Factor

Apart from the dominant isoform Munc13-1, Munc13-2 is the only other Munc13 protein expressed in mouse hippocampus (Augustin et al., 1999a, 2001). In order to examine whether Munc13-1-independent synapses employ Munc13-2 as an alternative priming factor, we generated Munc13-2 knockout mice and crossed them with Munc13-1 knockouts to breed Munc13-1/2 double knockout. Munc13-2 knockouts express no Munc13-2 protein as determined by Western blotting, show no overt phenotypic changes, and exhibit normal brain cytoarchitecture and synaptic ultrastructure (not shown). Munc13-1/2 double knockouts, on the other hand, were very fragile and often born dead. All double mutants that were born alive died within 1 hr after birth. However, hippocampi from double knockout embryos and newborn pups showed normal cell density and cytoarchitecture (not shown). Therefore, we used embryonic (E18) double mutant mice and wild-type identical Munc13-2 knockout littermates as controls for culturing hippocampal neurons. Neurons of double knockouts developed normally, as judged from morphological inspections and immunostainings, but displayed no evoked synaptic responses when stimulated with action potentials ($n = 45$, not shown), indicating that the remaining release activity in Munc13-1 knockout neurons relies on the priming function of Munc13-2. To verify that the loss of synaptic transmission in double knockout cells is only due to the lack of Munc13 priming factors and not caused by additional developmental defects, we overexpressed both hippocampal Munc13 isoforms in the double knockout neurons using Semliki Forest Virus expression vectors (Ashery et al., 2000). Virus-mediated expression levels of the two Munc13-EGFP fusion proteins as estimated by integrating somatic fluorescence 24 hr after infection were not statistically different (237 $\pm$ 95 Units, $n = 11$, for Munc13-1 versus 242 $\pm$ 84 Units, $n = 10$, for Munc13-2). Overexpression of either Munc13 isoform rescued synaptic transmission in the otherwise release-incompetent Munc13-1/2 double knockout neurons with high efficiency (Figure 2). EPSC amplitudes of the wild-type-like Munc13-2 knockout neurons were 1.3 $\pm$ 0.3 nA ($n = 17$), while double knockout neurons overexpressing Munc13-1 and Munc13-2 showed EPSC amplitudes of 0.84 $\pm$ 0.14 nA ($n = 25$) and 0.78 $\pm$ 0.11 nA ($n = 32$), respectively (Figures 2A and 2B). Similar rescue efficiencies were observed in inhibitory neurons although a smaller number of cells was examined (Figures 2C and 2D). Thus, Munc13-1/2 double knockout, release-incompetent neurons can be rescued to a wild-type-like phenotype by reintroduction of Munc13 proteins. The fact that rescued EPSC amplitudes approach wild-type levels irrespective of the Munc13 isoform used shows that all preformed synapses accept both Munc13 proteins as a priming factor. This is remarkable because in wild-

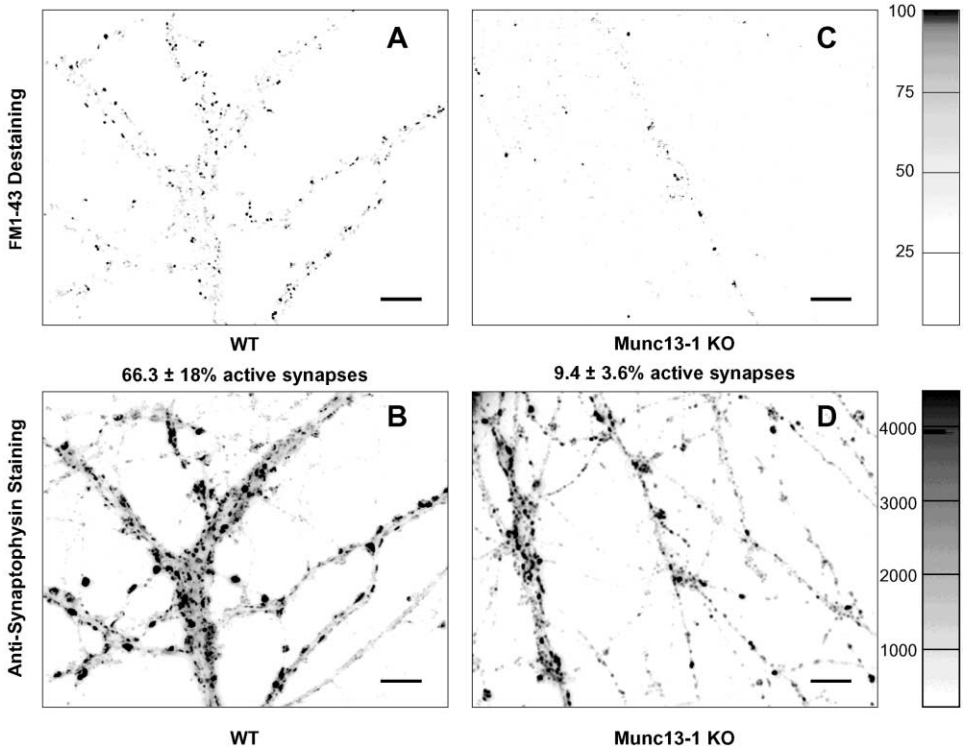

Figure 1. Distinct Pools of Synapses Employing Munc13-1 or Munc13-2 as Priming Factors

(A and C) Localization of active synapses in dendritic regions of autaptic neurons. Difference images representing specific FM1-43 destaining (see Experimental Procedures) were calculated in wild-type (A) and Munc13-1 knockout neurons (C).

(B and D) Localization of all synapses in the same cell regions as shown in (A) and (C). Neurons were stained with an antibody to Synaptophysin followed by a secondary Alexa-488 conjugated antibody.

The percentage of active synapses determined for glutamatergic wild-type (n = 18 cells) and Munc13-1 knockout cells (n = 12 cells) were calculated by dividing the number of synapses that stained with the antibody to Synaptophysin and stained/destained with FM1-43 by the total number of Synaptophysin-positive synapses in the same region. Bar: 15 μm.

type neurons, 90% of all synapses are exclusively dependent on Munc13-1 and therefore do not express Munc13-2 (Augustin et al., 1999b). In summary, these data demonstrate that in hippocampal primary neurons, Munc13-1 and Munc13-2 are expressed in different synapse populations formed by the same axon.

Munc13-1-Dependent and Munc13-2-Dependent Synapses Exhibit Different Types of Short-Term Synaptic Plasticity *during* High-Frequency Stimulation

Next we compared the release properties of wild-type synapses (that employ mainly Munc13-1 as a priming factor) and synapses from Munc13-1 knockout neurons (that employ Munc13-2 as a priming factor, see above). Reproducing our previous observations, we found that at low stimulation frequencies (0.2 Hz), EPSCs measured in Munc13-1 knockout neurons are dramatically reduced (107 ± 17 pA, n = 56, versus 1.28 ± 0.25 nA, n = 45, in wild-type or heterozygous mutant neurons; see also Augustin et al., 1999b). Munc13-2-dependent synapses release transmitter with an apparently wild-type-like release probability when stimulated at low frequency (Augustin et al., 1999b). However, they were found to differ profoundly from Munc13-1 synapses when stimulated at higher frequencies. Typically, EPSCs in wild-type, Munc13-1-dependent synapses depress with time when stimulated at frequencies between 1 and 20 Hz. At 10 Hz, EPSC amplitudes of wild-type neurons decreased steadily over 100 stimuli to 32% of the initial amplitude (1170 ± 250 pA to 373 ± 121 pA, n = 24; Figure 3A). EPSCs of Munc13-1 knockout neurons decreased wild-type-like for the first two consecutive responses (Figure 3D). However, the EPSC amplitude then increased to about 200% of the baseline value during ten stimuli (from 78 ± 16 pA to 147 ± 15, n = 47). After 100 stimuli, the EPSC amplitude in Munc13-1 knockout cells was still 70% larger than the initial amplitude (121 ± 15 pA, n = 47; Figure 3B). Despite this strongly augmenting behavior of Munc13-1 knockout neurons, the steady state amplitude of EPSCs during high-frequency stimulation remained below 30% of the wild-type value (Figure 3A). Because this remaining release component in Munc13-1 knockout neurons is not detectable in the completely release-incompetent Munc13-1/2 double knockout neurons, we conclude that it is maintained by Munc13-2-mediated vesicle priming. In contrast to glutamatergic cells, GABAergic Munc13-1 knockout cells showed more wild-type-like depression of IPSCs during 10 Hz stimulation (2.0 ± 0.5 nA to 0.36 ± 0.092 nA, n = 10, for wild-type cells and 2.12 ± 0.34 nA to 0.64 ± 0.11 nA, n = 27, for Munc13-1 knockout cells; Figure 3C). This

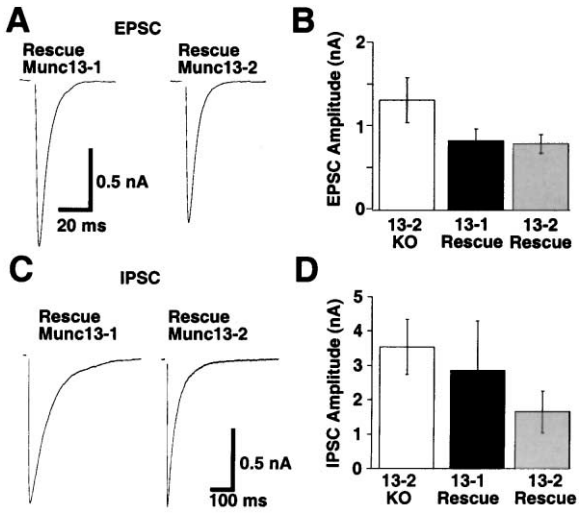

Figure 2. Rescue of EPSCs and IPSCs in Munc13-1/2 Double Knockout Neurons by Virus-Mediated Overexpression of Munc13-1 or ubMunc13-2

(A and C) Typical EPSC (A) and IPSC (C) from Munc13-1/2 double knockout neurons following virus-mediated overexpression of Munc13-1 or Munc13-2. Munc13-1/2 double knockout neurons had no evoked IPSCs or IPSCs (not shown).

(B and D) Mean EPSC (B) and IPSC (D) amplitudes from wild-type like Munc13-2 knockout neurons (white bars), and from Munc13-1/2 double knockout neurons after virus-mediated overexpression of Munc13-1 (black bar) or Munc13-2 (gray bar).

Error bars in this and following figures indicate standard error.

finding supports our previous observation (Augustin et al., 1999b) that loss of Munc13-1 has little effect on inhibitory neurotransmission, most likely because Munc13-2 is coexpressed with Munc13-1 in all GABAergic synapses.

To verify that the augmenting phenotype in Munc13-1 knockout neurons is strictly coupled to the presence of Munc13-2 and not due to culture artifacts (the neurons have 90% less active synapses than wild-type neurons), we examined Munc13-1/2 double knockout neurons after Semliki Forest Virus-mediated reintroduction of Munc13-1 or ubMunc13-2. Cells rescued with the ubMunc13-2 isoform showed the EPSC augmentation during 10 Hz stimulation that is characteristic of Munc13-1 knockout neurons in which Munc13-2 is assumed to drive vesicle priming (compare Figures 3B and 3E). Conversely, cells rescued with the Munc13-1 isoform showed a depression of EPSC amplitudes during 10 Hz stimulation that is typically seen in wild-type and Munc13-2 knockout cells (compare Figures 3B and 3E). Thus, overexpression of Munc13-1 or ubMunc13-2 in Munc13-1/2 double knockout, priming-incompetent hippocampal neurons creates phenocopies of wild-type/Munc13-2 knockout and Munc13-1 knockout neurons, respectively. Synaptic release activity in wild-type or Munc13-2 knockout cells is therefore driven by Munc13-1 while synaptic transmitter release in Munc13-1 knockout cells is due to the priming action of Munc13-2 only. The striking differences in short-term plasticity between wild-type and Munc13-1 knockout neurons (Figure 3 and additional data below) are due to intrinsic functional differences between Munc13-1 and

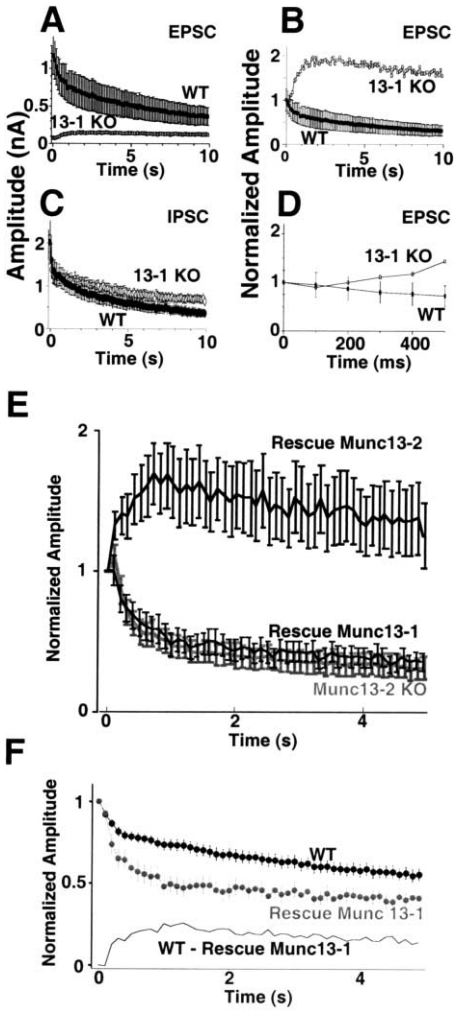

Figure 3. Depression and Delayed Facilitation of EPSCs during Action Potential Trains in Munc13-1- and Munc13-2-Dependent Synapses

(A and B) Absolute (A) and normalized (B) synaptic responses from excitatory wild-type and Munc13-1 knockout cells during a 10 Hz train (10 s). Wild-type EPSCs (wild-type, black circles) show about 70% depression after 100 evoked responses. EPSCs in Munc13-1 knockout cells are much smaller than wild-type signals, but increase to 170% of the initial amplitude.

(C) Normalized IPSC amplitudes from wild-type (wild-type, black circles) and Munc13-1 knockout cells (white circles). IPSCs in both genotypes show about 70% depression after 100 evoked responses.

(D) Expanded time course of data shown in (B) to illustrate the delayed increase of EPSC amplitudes in Munc13-1 knockout cells beginning with the fourth EPSC.

(E) Normalized EPSC amplitudes during a 10 Hz train measured in Munc13-2 knockout, wild-type-like control neurons and in Munc13-1/2 double knockout cells overexpressing either Munc13-1 or ubMunc13-2.

(F) Comparison of amplitude time courses during 10 Hz train in wild-type (black circles, n = 21) and Munc13-1/2 double knockout cells overexpressing Munc13-1 (gray circles, n = 19). The black line is the calculated difference between the two groups and resembles the amplitude time course of the Munc13-2-dependent synapses (see Figures 3B and 3E). Note that the data sets of Figures 3A–3D and Figures 3E–3F were obtained in separate experiments.

Munc13-2, which differentially control changes in release dynamics during high-frequency action potential trains.

In wild-type cells, Munc13-2 synapses contribute weakly but significantly to the maintenance of synaptic

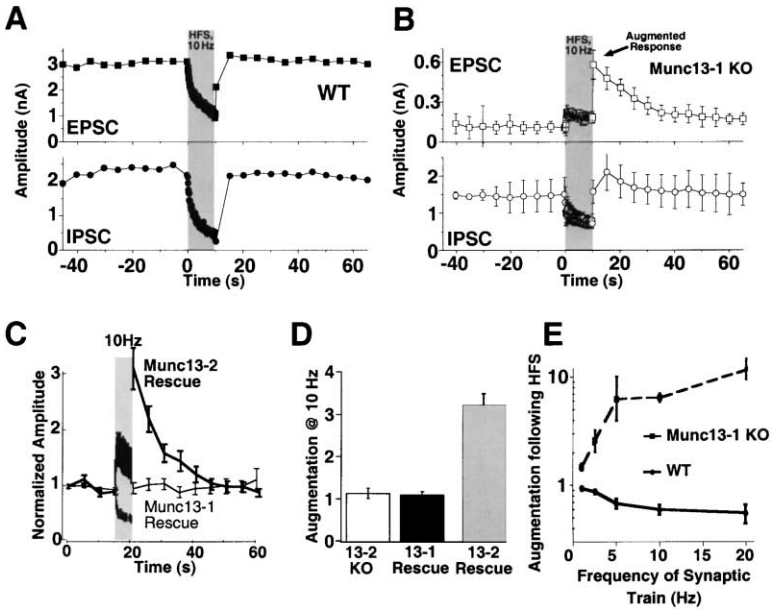

Figure 4. EPSC Amplitudes in Munc13-1 Knockout, Munc13-2-Dependent Synapses Are Augmented following Action Potential Trains

(A and B) Average absolute EPSCs (top) and IPSCs (bottom) before, during (gray area), and after a 10 Hz train (50 stimuli) in wild-type (A) and Munc13-1 knockout cells (B). To determine augmentation ratios, augmentation of the EPSC was measured 2 s after the train.

(C) Normalized EPSCs showing depression and augmentation following a 10 Hz action potential train (50 stimuli) in Munc13-1/2 double knockout neurons overexpressing Munc13-1 (bottom trace) or Munc13-2 (top trace), respectively.

(D) Average augmentation in Munc13-2 knockout, Munc13-1-dependent, wild-type-like control neurons (white bar, n = 17), and in Munc13-1/2 double knockout neurons overexpressing Munc13-1 (black bar, n = 24) or ubMunc13-2 (gray bar, n = 29).

(E) Average augmentation of EPSCs in wild-type (black squares) and Munc13-1 knockout cells (black circles) as a function of the train frequency (1 Hz, 20 stimuli; 2.5 Hz, 40 stimuli; 5 and 10 Hz, 50 stimuli; 20 Hz, 100 stimuli). Measurements are from 17–45 cells. Logarithmic y axis.

responses. Closer examination of the degree of depression during 10 Hz trains in wild-type neurons and Munc13-1/2 double knockout cells overexpressing Munc13-1 revealed that double knockout neurons rescued with Munc13-1 depressed more strongly than wild-type cells (Figure 3F). The time course of the computed difference amplitude between wild-type and Munc13-1 rescue after normalization had a shape that was similar to the one obtained in Munc13-2-dependent synapses, indicating additivity of the two synapse populations.

Munc13-1- and Munc13-2-Dependent Synapses Exhibit Different Types of Short-Term Synaptic Plasticity *following* High-Frequency Stimulation

In order to determine which release parameters are differentially affected by Munc13-1 and Munc13-2 during high-frequency action potential trains, we examined synaptic amplitudes (stimulation at 0.2 Hz) immediately after a 10 Hz action potential train. We found that in wild-type neurons, EPSCs (n = 27) and IPSCs (n = 18) recovered from depression to baseline values within one or two post train stimuli (Figure 4A). In striking contrast, glutamatergic Munc13-1 knockout neurons showed a dramatic increase of EPSC amplitudes 2 s following the 10 Hz train, reaching 578 ± 108 pA (n = 45) which represents a more than 5-fold augmentation over basal EPSC amplitudes (Figure 4B). GABAergic Munc13-1 knockout cells also showed a significant, albeit much more subtle, degree of IPSC augmentation (Figure 4B, bottom), providing the first evidence for an effect of the Munc13-1 knockout on GABAergic neurons (see Augustin et al., 1999b). Here, the baseline amplitude was 1.45 ± 0.43 nA, and following the 10 Hz action potential train, amplitudes were augmented to 2.09 ± 0.49 nA (n = 12).

In order to verify that the differences in post train EPSC augmentation between wild-type and Munc13-1 knockout neurons are really due to functional differences between Munc13-1 and Munc13-2, which drive vesicle priming in the respective neurons, we employed rescue experiments with Munc13-1/2 double knockout neurons. As with short-term plasticity characteristics *during* high-frequency action potential trains, we found that overexpression of Munc13-1 generated a phenocopy of nonaugmenting wild-type/Munc13-2 knockout cells while overexpression of ubMunc13-2 resulted in an EPSC augmenting phenotype that closely resembled that of Munc13-2-driven Munc13-1 knockout neurons (Figures 4B–4D). These data demonstrate that wild-type or Munc13-2 knockout neurons serve as ideal models to study Munc13-1-mediated vesicle priming, while Munc13-1 knockout neurons allow the analysis of Munc13-2 function in isolation. The differences in short-term plasticity of synaptic transmission between wild-type and Munc13-1 knockout neurons are mainly, if not exclusively, due to functional differences between Munc13-1 (depressing) and Munc13-2 (augmenting). The post train EPSC augmentation in Munc13-2 synapses is transient (Figures 4B top and 4C), and augmented EPSCs returned to baseline with a time constant of 5–18 s (8.3 ± 2.1 s; n = 45). These characteristics (identical basal release probability, delayed onset of amplitude increase, time course of decay to baseline) are consistent with forms of short-term plasticity that are classically defined as augmentation (Zucker, 1989). Therefore, we used Munc13-2-dependent synaptic transmission in Munc13-1 knockout neurons as a model for the analysis of augmentation mechanisms.

Munc13-2-Dependent Synapses as a Model for Augmentation

To detect a possible postsynaptic contribution to the augmentation observed in Munc13-1 knockout, Munc13-2-dependent cells, we first compared augmen-

tation of the slow NMDA component of the EPSC with the fast AMPA component. To measure both components simultaneously, EPSCs were stimulated in the presence of 10 μM glycine and 2.7 mM Ca^{2+} but in the absence of Mg^{2+}. The transmitter release probability under these conditions was slightly higher than under our standard conditions (4 mM Ca^{2+}/4 mM Mg^{2+}). Augmentation was induced with a 10 Hz action potential train, and the dual component EPSC was examined before and 2 s after augmentation. Presumably due to the elevated release probability, augmentation was generally less pronounced than under standard ionic conditions, but the degree of augmentation was indistinguishable between the AMPA (2.4- ± 0.2-fold, n = 14) and NMDA components (2.57- ± 0.13-fold, n = 9) (not shown). In additional experiments, we tested for potential changes in postsynaptic sensitivity during augmentation (e.g., due to postsynaptic insertion of new receptors) by probing the total responsiveness of postsynaptic AMPA receptors in Munc13-2-dependent cells. We expected that this approach would allow us to reliably detect increases in postsynaptic receptor density or sensitivity due to augmentation because a large fraction of cellular AMPA receptors is synaptically localized (Craig and Boudin, 2001) and an average EPSC augmentation of some 500% would therefore be paralleled by a readily detectable increase in cellular responses to exogenously added AMPA receptor agonists. However, when we compared responses of Munc13-1 knockout, Munc13-2-dependent cells to exogenously applied kainate (10 μM) before and after induction of augmentation, we found that induced responses were not changed (103% ± 1%, n = 7). Thus, a postsynaptic contribution to the augmentation seen in Munc13-2-dependent neurons can be excluded.

We next quantified the vesicle supply/consumption balance by examining augmentation as a function of train frequency (1–20 Hz). At all stimulation frequencies, Munc13-1-dominated wild-type neurons showed depression, and the degree of depression increased with the train frequency as expected (Figure 4E). In Munc13-1 knockout, Munc13-2-driven synapses, however, the degree of augmentation generally increased with train frequency. At a stimulation frequency of 1 Hz, we measured 50% augmentation, and at 20 Hz, augmentation reached 1120% ± 210% (n = 7) of the basal amplitude. The lack of any form of depression and almost linear increases of augmentation with vesicular consumption in Munc13-2-driven synapses suggests that, in contrast to the wild-type situation, vesicular supply is not the rate-limiting step for synaptic release in Munc13-2-driven synapses.

Augmentation Is Mediated by an Increase of the Readily Releasable Vesicle Pool Size and the Vesicular Release Probability

Synaptic depression in wild-type neurons has been interpreted as depletion of the RRP because pool sizes and synaptic responses are reduced in parallel during high-frequency stimulation. Accordingly, recovery from such depression is thought to reflect refilling of a partially depleted vesicle pool (Rosenmund and Stevens, 1996; Wang and Kaczmarek, 1998). To examine whether the pronounced augmentation in Munc13-2-dependent synapses during high-frequency stimulation is caused

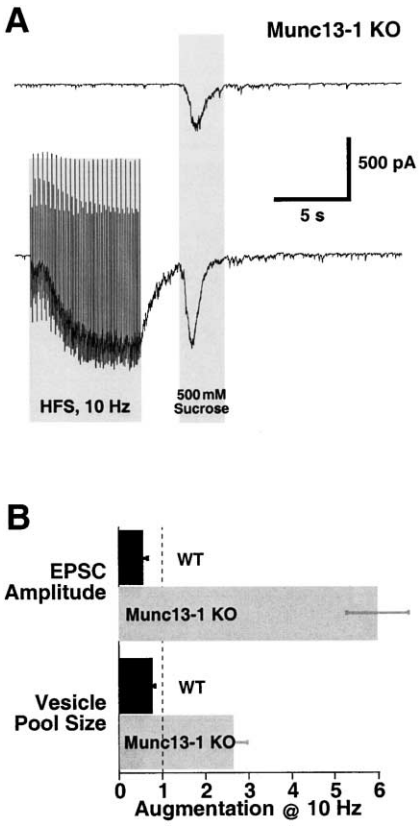

Figure 5. Augmentation Is Accompanied by an Increase of the Readily Releasable Vesicle Pool and of the Vesicular Release Probability

(A) Two current responses to hypertonic sucrose stimulation (3 s, 500 mOsm added to the external medium, gray area) from the same excitatory Munc13-1 knockout neuron before (top) and immediately after (bottom) a 10 Hz action potential train.

(B) Bar graph showing the average synaptic augmentation and pool size change following the 10 Hz train for wild-type (black bars) and Munc13-1 knockout neurons (gray bars). Data were normalized to the control EPSC/pool size measurement. Dotted line indicates the size of the control EPSC/pool size.

by an increase in the size of the RRP, we determined pool sizes during augmentation. Although augmentation is transient, its decay time constant of approximately 8 s allowed us to estimate the pool size during the augmented state by applying hypertonic sucrose solution 2 s after the induction of augmentation (Figure 5A). Hypertonic sucrose solution releases the entire RRP within 3 s in a Ca^{2+}-independent manner. The total charge integrated over the transient part of the inward current induced by the hypertonic solution represents the size of the RRP (Rosenmund and Stevens, 1996). Knowing the average charge produced by a single mEPSC, the number of vesicles in the RRP can be determined. For nonaugmented Munc13-2-dependent synapses in Munc13-1 deletion mutant cells, the total pool size summed over all autapses of a neuron was 275 ± 34 vesicles. In contrast, 2 s following a 10 Hz/7 s action potential train, the size of the RRP had increased by 265% ± 40% to 730 ± 110 vesicles (n = 12; Figure 5B, bottom). Under the same conditions, wild-type neurons showed a 25% ± 4% decrease in RRP size from 3120 ±

450 vesicles before the 10 Hz train to 2355 ± 340 after the train (n = 10). Parallel measurements of EPSC amplitudes before and after a 10 Hz train showed an increase of 600% ± 71% in Munc13-2-dependent synapses (n = 35; Figure 5B, top), which is larger than the increase observed for the RRP sizes (265% ± 40%; Figure 5B, bottom). On the other hand, evoked amplitudes of wild-type neurons decreased by 41% ± 8% (n = 7; Figure 5B, bottom). These data demonstrate that high-frequency stimulation of Munc13-2-dependent synapses primes a pool of vesicles that is reluctant to be primed at low stimulation frequencies. In addition, synaptic responses from Munc13-2-dependent synapses augment more strongly than the pool size itself (600 ± 71 versus 265% ± 40%), demonstrating that the vesicular release probability immediately after induction of augmentation is also increased approximately 2-fold, which is most likely due to the elevated intraterminal Ca^{2+} concentration and thus represents a facilitation component.

Instead of a change in release probability and RRP size as an underlying mechanism of augmentation, high-frequency stimulation may lead to a "reawakening" of previously silent synapses. To examine whether such reawakening occurs, we irreversibly blocked NMDA receptors of active synapses in Munc13-1 knockout, Munc13-2-dependent neurons at low stimulation frequencies using pharmacological means and subsequently tested for a transient appearance of a new synapse population following a 10 Hz train. EPSCs were stimulated in the presence of 10 μM glycine and 2.7 mM Ca^{2+} but in the absence of Mg^{2+}. The slow NMDA receptor component of EPSCs can be blocked specifically, completely, and irreversibly by repeated stimulation of synaptic release in the presence of the open NMDA receptor channel blocker MK-801. Consequently, an induction of augmentation via synapse reawakening should induce a large de novo NMDA EPSC component if a population of previously silent synapses reawakened during the augmentation-inducing 10 Hz train. The NMDA component of EPSCs was blocked by evoking 120 NMDA EPSCs (0.2 Hz) in the presence of 5 μM MK-801. This led to a reduction of the NMDA EPSC component by more than 90%. Following washout of MK-801, the synaptic amplitudes of both AMPA (fast component) and NMDA components (slow component) of EPSCs were monitored before and after a 10 Hz train (7 s). Following a 10 Hz train, the AMPA-mediated component of EPSCs transiently increased as expected (n = 6, Figures 6A–6C). However, apart from the expected augmentation of the minute remaining NMDA component, a new substantial NMDA-mediated component did not appear (Figures 6B and 6C). This demonstrates (1) that the synapses mediating the augmentation in Munc13-1 knockout, Munc13-2-driven neurons are the same synapses that are active at low stimulation frequencies, (2) that augmentation is restricted to the Munc13-2-dependent synapse population, and (3) that synapse reawakening does not contribute to the observed augmentation in Munc13-1 knockout cells.

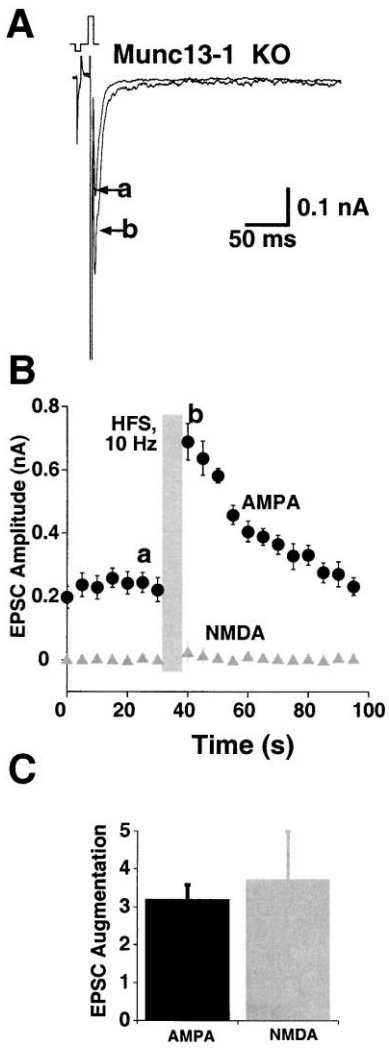

Figure 6. Augmentation Is Not Due to a Reawakening of Silent Synapses

Synaptic NMDA EPSCs were initially blocked in Munc13-1 knockout cells by a series of EPSCs stimulated at low stimulation frequency (0.2 Hz) in the presence of 5 μM MK-801.

(A) Dual component EPSCs after washout of MK-801 at time points immediately preceding (a) or following (b) the 10 Hz train (7 s) are shown for an example neuron. The remaining slow NMDA component of the EPSC augmented not more than expected.

(B) Time course of averaged AMPA and NMDA mediated amplitudes before and after the 10 Hz train (gray area).

(C) Average augmentation of the remaining NMDA (gray bar) and the AMPA component (black bar) 2 s following the 10 Hz train compared to the control period preceding the train (n = 6).

Augmentation Is Triggered by Elevation of the Intracellular Ca^{2+} Concentration

High action potential frequencies lead to an increase of the basal intraterminal Ca^{2+} concentration by several hundred nM (Helmchen et al., 1996). This rise in the Ca^{2+} concentration may be an important factor in short-term plastic changes of transmitter release. Consequently, the augmentation observed in Munc13-1 knockout, Munc13-2-dependent synapses following high-frequency stimulation may be mediated by elevated levels of the intraterminal Ca^{2+} concentration. In this case, similar degrees of augmentation should be observed following increases of the intraterminal Ca^{2+} concentration due to manipulations that do not involve the induction of action potentials.

We elevated the intraterminal Ca^{2+} concentration in-

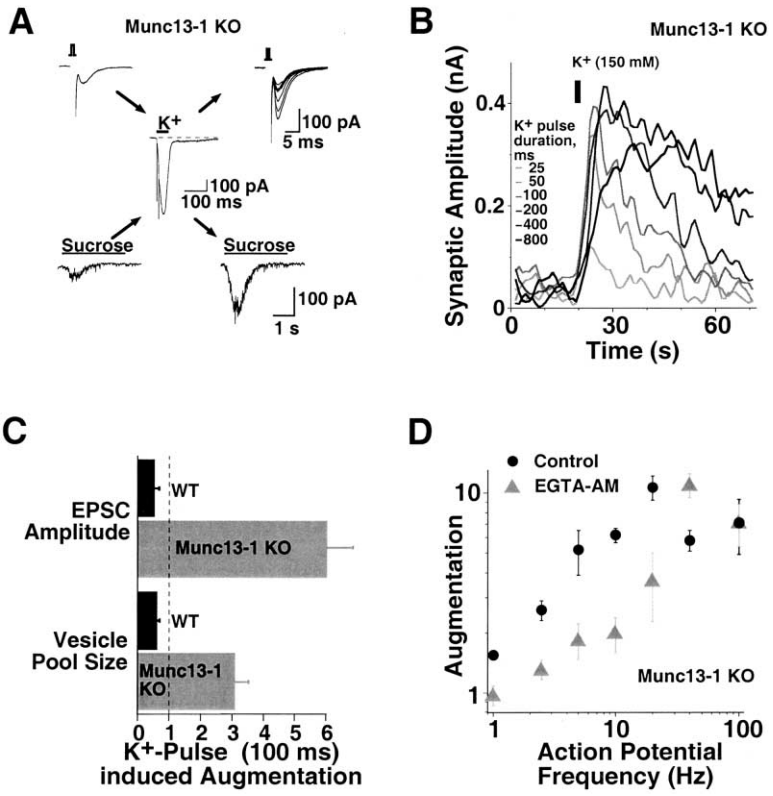

Figure 7. Augmentation Depends on Increases of the Intracellular Ca^{2+} Concentration

(A) Synaptic (upper row) and sucrose induced (lower row) EPSC responses from a Munc13-1 knockout neuron before (left side) and after (right side) a 100 ms application of 150 mM KCl (in standard external solution) to the entire neuron (middle). The KCl application induced a somatic inward current, presumably due to the opening of inward rectifier K^+ channels, and was usually accompanied by several unclamped spikes. The tail current following the K^+ pulse was reminiscent of massive mEPSC activity due to activation of voltage-dependent Ca^{2+} channels in the unclamped nerve terminal population. The right side of the panel shows the transient augmentation of the synaptic response seen in the series of EPSCs recorded at 0.2 Hz (top right) and the increase of the vesicle pool 2 s following the K^+ pulse (bottom right).

(B) Augmentation of EPSC amplitudes (measured at 1 Hz) in a Munc13-1 knockout neuron induced by K^+ pulses of increasing duration (150 mM; 25, 50, 100, 200, 400, 800 ms; from light gray to black traces). Augmentation was maximal with a 100 ms pulse. Longer pulses led to delayed (due to pool depletion) and longer lasting augmentations. Similar observations were made in five additional cells.

(C) Bar plot showing the degree of modulation of the synaptic response and pool size in wild-type and Munc13-1 knockout glutamatergic neurons by a 100 ms K^+ pulse (150 mM, 4 mM external Ca^{2+}).

(D) Increased presynaptic Ca^{2+} buffering reduces frequency-dependent augmentation. Action potential frequency/augmentation profile from control (black circles) and EGTA-AM treated (gray triangles) Munc13-1 knockout neurons. Augmentation in EGTA-AM treated cells was consistently lower for frequencies of 1–20 Hz. Numbers of stimuli were as given in Figure 2E; 40 Hz, 100 stimuli; 100 Hz, 100 stimuli. Measurements are from 5–12 cells. Control data set is identical to Figure 9B.

dependently of action potentials by external application of short K^+ pulses (65–150 mM, 0.025–0.8 s) in the presence of 4 mM external Ca^{2+}. This K^+ application should lead to a depolarization of unclamped terminals and to an opening of presynaptic voltage-dependent Ca^{2+} channels, which in turn would result in an increase of the intraterminal Ca^{2+} concentration and augmentation. We first examined the dose dependency and time course of augmentation in response to K^+ induced depolarizations. Short pulses (25–800 ms) of isotonic K^+ (150 mM) in the presence of 4 mM Ca^{2+} were applied to Munc13-1 knockout, Munc13-2 dependent neurons, and synaptic amplitudes were monitored at 1 Hz resolution (Figure 7B). Particularly at short pulse duration (25–100 ms), augmentation developed within the first few synaptic responses, suggesting that Ca^{2+} is able to transform reluctantly primed vesicles into fusion-competent vesicles within a few seconds. After longer lasting depolarizations (200–800 ms), the degree of augmentation was smaller and its time course slowed down, presumably due to significant depletion of vesicles from the RRP during the depolarization and longer lasting and larger Ca^{2+} elevations in the terminal. These data suggest that the Ca^{2+}-dependent process underlying augmentation develops very rapidly (1–2 s), making an involvement of certain biochemical processes such as phosphorylation less likely.

To quantify the degree of EPSC and pool augmentation, we chose the briefest K^+ pulse that caused maximal augmentation (150 mM external K^+ for 100 ms) and compared EPSCs and sucrose responses before and after the K^+ pulse. Both synaptic responses (603% $\pm$ 85%, n = 32) and the size of hypertonically induced responses (312% $\pm$ 41%, n = 6) increased dramatically upon K^+ stimulation (Figures 7A and 7C). In a given cell, K^+-induced augmentation correlated directly with the augmentation seen after 10 Hz trains of action potentials (EPSC amplitude: 587% $\pm$ 53%, n = 12; pool size: 262% $\pm$ 43%, n = 5; see also Figure 5). In contrast to Munc13-1 knockout, Munc13-2-dependent cells, wild-type neurons showed depression of both synaptic amplitude (to 57% $\pm$ 12%, n = 14) and pool size (to 64% $\pm$ 6%, n = 14, not shown) following the K^+ pulse, again closely resembling the measurements obtained with trains of action potentials (Figure 5).

Above data demonstrate that K^+ pulses mimic the effects of high-frequency stimulation in Munc13-1 knockout, Munc13-2-dependent synapses, suggesting that in both cases, Ca^{2+} elevation in Munc13-1 knockout synapses is responsible for the observed augmentation. To test this further, we compared the stimulation frequency dependence of augmentation in Munc13-1 knockout, Munc13-2 synapses under standard conditions with cells that were pretreated with the membrane-permeable derivative of the Ca^{2+} chelator EGTA, EGTA-AM (50 μM, 20 min, 37°C). This treatment increases the

Ca^{2+} buffering capacity in presynaptic terminals significantly and therefore lowers the intraterminal Ca^{2+} elevations during action potential trains. Although not quantified, the synaptic EPSC amplitudes at low-frequency stimulation rates were smaller in EGTA pretreated cells as compared to untreated cultures, indicating the presence of significant EGTA concentrations in presynaptic terminals. As shown in the frequency-augmentation profile (Figure 7D), augmentation was shifted in the EGTA-AM pretreated cells at frequencies below 40 Hz ($p < 0.02$ at all frequencies tested, except 100 Hz). At 10 Hz, untreated Munc13-2-dependent cells augmented 6.17 $\pm$ 0.51-fold ($n = 29$), while EGTA-AM treated cells augmented only 2.0- $\pm$ 0.4-fold ($n = 8$, $p < 0.0002$). Augmentation in untreated Munc13-2-dependent cells reached a maximum (>10-fold) at around 20 Hz, while at 40 and 100 Hz, augmentation was submaximal (5- to 7-fold), which correlates nicely with the submaximal augmentation induced by K^+ pulses with a duration above 200 ms (Figure 7B). EGTA-treated Munc13-2-dependent cells reached maximal augmentation (11.0- $\pm$ 1.5-fold, $n = 8$) at a higher frequency (40 Hz) than untreated cells but showed a similar degree of augmentation at 100 Hz, further demonstrating that, presumably due to buffer saturation, higher train frequencies are needed to reach full augmentation.

Our data on the effects of EGTA-AM support the conclusion that Ca^{2+} elevation in Munc13-1 knockout, Munc13-2-dependent synapses is responsible for the observed augmentation. In the case that their function is different at the final Ca^{2+}-triggered step of exocytosis, this can be shown by examining the Ca^{2+} dependency of evoked release at low stimulation frequencies. We studied this by measuring EPSCs in the presence of systematically varying external Ca^{2+} concentrations. Application of an external solution containing 4 mM Ca^{2+} and 4 mM Mg^{2+} was alternated with application of external solutions containing lower or higher Ca^{2+} concentrations and a constant Mg^{2+} concentration. EPSCs at varying Ca^{2+} concentrations were measured and normalized to the response seen with the standard external solution containing 4 mM Ca^{2+} and 4 mM Mg^{2+}. We did not find any evidence for a difference in Ca^{2+} dependency of release between wild-type ($n = 6$–32) and Munc13-1 knockout, Munc13-2-dependent synapses ($n = 11$–43, not shown). Thus the last, Ca^{2+}-triggered fusion step in synaptic transmitter release is not the process that is differentially regulated by Munc13 isoforms.

Ca^{2+}-Induced Augmentation Requires Phospholipase C Activity

In neuroendocrine cells and hippocampal neurons, concomitant action of PKC and Ca^{2+} can increase the size of the RRP (Gillis et al., 1996; Stevens and Sullivan, 1998; Smith et al., 1998). We therefore used pharmacological tools to examine whether Ca^{2+} mediates augmentation in Munc13-2-dependent synapses via Ca^{2+}-dependent kinases or phosphatases or through modifications of the actin cytoskeleton (Figure 8A). Application of the PKCγ blocker GÖ-6973 (100 nM) or of the (at this concentration) more unspecific kinase blocker staurosporine (100 nM) failed to suppress augmentation. Likewise, a cocktail of phosphatase inhibitors containing

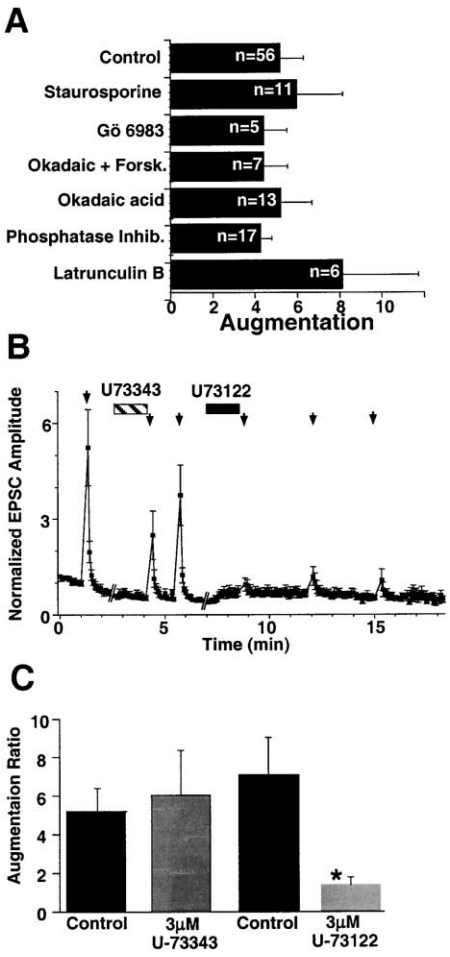

Figure 8. Augmentation Depends on Phospholipase C

(A) Bar diagram showing the degree of EPSC augmentation in Munc13-1 knockout cells in the absence (control) or presence of various drugs. Following induction of augmentation (10 Hz) at control conditions, the cells were pretreated with the indicated drug for 150–300 s, and augmentation was measured again. Blockers of kinases and phosphatases (cypermethrin, 1 nM; calyculin A, 10 nM; cyclosporine, 1 μM), and blockers of actin polymerization (latrunculin B; 10 μM), were ineffective in blocking augmentation. Likewise, a combination of forskolin (1 μM) with the phosphatase 2A inhibitor okadaic acid (1 μM) or okadaic acid alone (1 μM) were unable to block augmentation.

(B) Average normalized EPSC amplitude from Munc13-1 knockout glutamatergic neurons ($n = 8$) are plotted against time of recording. At points indicated by the arrows, augmentation is induced by a 10 Hz stimulus (5 s). Bars indicate the time when either the inactive (U73343, 3 μM, 150 s) or the active (U73122, 3 μM, 150 s) was applied to the bath. Only treatment with the PLC inhibitor U73122 (3 μM), but not its inactive analog U73445 (3 μM), inhibited the induction of augmentation.

(C) Mean augmentation ratios from the first (control), second (following U73343 incubation), third (control), and fourth induction (following U73122 incubation, *, significance < 0.05) of augmentation. Same data set as (B).

cypermethrin (1 nM), calyculin A (10 nM), and cyclosporine A (1 μM), or okadaic acid (1 μM) alone did not alter augmentation. Similar results were obtained with forskoline treatment (1 μM), which leads to increased intracellular cAMP levels. Moreover, the membrane permeable inhibitor of actin polymerization, latrunculin B (10 μM),

also failed to affect augmentation. Thus, the augmentation observed in Munc13-2-dependent synapses following high-frequency stimulation is unlikely to be due to Ca^{2+}-dependent changes in the function of the actin cytoskeleton or in phosphorylation or dephosphorylation reactions that may modify proteins relevant for vesicle priming or release. However, because above data are essentially negative in nature, additional experiments will be necessary to unequivocally exclude an involvement of kinases, phosphatases, or the cytoskeleton in the augmentation of Munc13-2-dependent synapses.

Munc13-1 contains a diacylglycerol/β-phorbol ester binding C_1 domain that is responsible for the fast β-phorbol ester induced synaptic potentiation in hippocampal neurons as well as for the maintenance of synaptic responses during trains of action potentials (Rhee et al., 2002). To test whether the differences between Munc13-1 and Munc13-2 with respect to their role in short-term plasticity are caused by differences in a C_1 domain-induced signaling cascade, we inhibited the production of the Munc13 C_1 domain ligand, diacylglycerol, using the specific PLC inhibitor U73122. Preincubation of Munc13-1-deficient, Munc13-2-dependent cells with U73122 at 3 μM for 150 s led to an almost complete inhibition of augmentation, but left basal release essentially unaffected (Figures 8B and 8C). The inactive analog U73343 (3 μM), however, failed to modify augmentation. Thus, PLC activity and the presence of diacylglycerol is required for induction of augmentation, presumably acting on the C_1 domain of Munc13s.

Potentiation of Transmitter Release by β-Phorbol Esters Correlates with Differential Augmentation of Munc13 Isoforms

Stable analogs of diacylglycerol, the β-phorbol esters, are known to activate PKC and Munc13-1 (Betz et al., 1998). The fact that diacylglycerol is required for the induction of augmentation in Munc13-2-dependent synapses suggests that augmentation is linked to the activation of the Munc13-2 C_1 domain. We therefore examined whether the β-phorbol ester sensitivities of Munc13-1- and Munc13-2-dependent synapses differ in a similar manner as their depression/augmentation properties. We found that the β-phorbol ester (PDBU) induced EPSC potentiation in Munc13-1 knockout, Munc13-2-dependent cells was much larger than that seen in Munc13-1-dominated wild-type cells. Synaptic potentiation upon application of PDBU (100–1000 nM) was 570% ± 118% (n = 12) in Munc13-2-dependent synapses and 199% ± 25% (n = 7) in Munc13-1-dominated wild-type synapses (Figure 9A). To confirm that the different degree of PDBU-induced potentiation is strictly dependent on the respective Munc13 isoform expressed, we used Semliki Forest Virus rescue experiments in Munc13-1/2 double knockout neurons. In neurons rescued with ubMunc13-2, PDBU application caused an EPSC potentiation of 510% ± 83% (n = 11). In contrast, EPSCs in neurons rescued with Munc13-1 were potentiated by 247% ± 22% (n = 12, Figure 9C). Thus, the degree to which β-phorbol esters potentiate transmitter release is dependent on the respective Munc13 isoform expressed, as is the case with train-induced augmentation. Furthermore, PDBU-induced potentiation and train-induced augmentation were not additive (Figure 9B). Frequency-augmentation profiles from Munc13-2-dependent cells in the absence or presence of 1 μM PDBU showed that at frequencies at or above 20 Hz, untreated Munc13-2-depen-

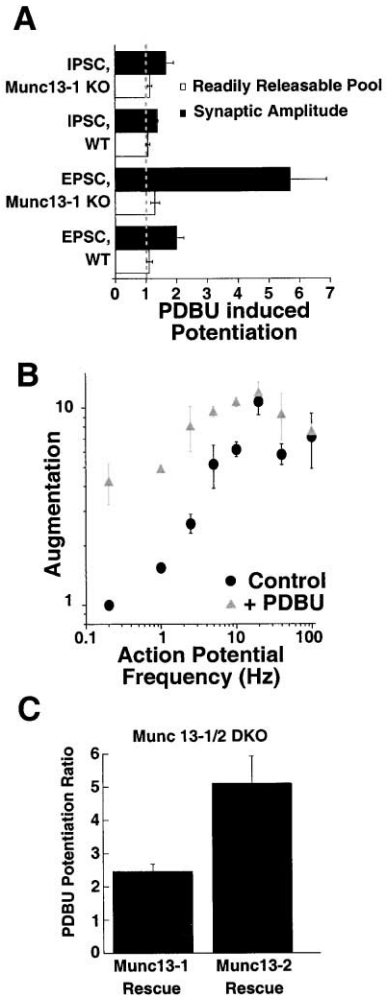

Figure 9. Munc13-Isoform-Dependent Regulation of Release by β-Phorbol Esters

(A) Effects of the β-phorbol ester PDBU (1 μM, 60 s) on synaptic (wild-type, n = 9; knockout, n = 17) and sucrose (wild-type, n = 8; knockout, n = 11) induced IPSC and synaptic (wild-type, n = 7; knockout, n = 17) and sucrose (wild-type, n = 4; knockout, n = 5) induced EPSC responses in wild-type and Munc13-1 knockout neurons. Synaptic and sucrose induced responses were normalized to control responses measured before PDBU application. Dashed line indicates the control value.

(B) Nonadditivity of action potential train-induced augmentation and β-phorbol ester-induced potentiation in Munc13-1 knockout neurons. Action potential frequency/augmentation profile from Munc13-1 knockout neurons in the absence (Control, black circles) or presence of PDBU (1 μM, gray triangles). Data for PDBU-treated cells were normalized to the basal EPSC amplitude measured before treatment. EPSC augmentation in untreated and treated synapses reached similar values for frequencies at and above 20 Hz. Numbers of stimuli were as given in Figure 7D. Measurements are from 4–12 cells.

(C) PDBU (1 μM) induced EPSC potentiation in Munc13-1/2 double knockout neurons that had been rescued by viral overexpression of Munc13-1 (n = 11) or Munc13-2 (n = 12).

dent synapses and PDBU-treated synapses reached similar degrees of augmentation. PDBU-induced potentiation of IPSCs was much less pronounced and differences between Munc13-1- and Munc13-2-dominated cells were very small (Figure 9A).

To examine whether the pronounced PDBU-induced EPSC increase in Munc13-2-dependent cells is due to an underlying increase in RRP, we examined changes in pool size in response to PDBU (see also Stevens and Sullivan, 1998). The RRP increased by 30% ± 15% (n = 5) in Munc13-2-dependent synapses and by 11% ± 5% in Munc13-1-dominated wild-type synapses (n = 4; Figure 9A). Thus, the strongly potentiating effect of PDBU on evoked transmitter release from Munc13-2-dependent cells is not caused by a correspondingly strong increase in the RRP size. This is in contrast to augmentation induced by high-frequency action potential trains, where pool size is strongly increased. These findings indicate that β-phorbol esters exert their effects through a mechanism that is only partially redundant with the mechanism of Ca^{2+}-induced augmentation, or that the β-phorbol esters induced increase of pool size requires an additional factor such as Ca^{2+}.

Discussion

Two Functional Classes of Synapses Defined by the Differential Localization of Synaptic Vesicle Priming Factors Munc13-1 and Munc13-2

We show that a single axon of an individual glutamatergic hippocampal neuron forms two classes of presynaptic terminals which can be distinguished by their equipment with the Munc13 priming factors Munc13-1 and Munc13-2, and by their short-term plasticity characteristics. Munc13-2-dependent synapses facilitate during trains of action potentials and show augmentation following high-frequency stimulation while Munc13-1-dependent synapses exhibit depression and no augmentation under the same stimulation conditions (Figure 3). Thus, Munc13s do not only act as essential vesicle priming factors (Aravamudan et al., 1999; Augustin et al., 1999b; Richmond et al., 1999), but differentially determine short-term plasticity properties of individual synapses. Despite this difference in short-term plasticity, basic properties of the two types of synapses, such as initial release probability (Augustin et al., 1999b) and Ca^{2+} sensitivity of release, are very similar. Overexpression experiments in Munc13-1/2 double knockout neurons demonstrate that preexisting synapses which would otherwise use Munc13-1 as priming factor and have a depressing phenotype can be equipped with Munc13-2 and acquire a facilitating/augmenting phenotype (Figure 3). This indicates that apart from the equipment with Munc13s, the molecular mechanism of release from the two types of Munc13-dependent glutamatergic synapses is identical, that their differences in short-term plasticity are only due to their differential equipment with Munc13-1 or Munc13-2, and that depressing and facilitating/augmenting characteristics are intrinsic features of the two Munc13 isoforms.

That individual axons in situ can form functionally different, facilitating and depressing synapses is evident from experiments in cortical (Reyes et al., 1998; Thomson, 1997) and hippocampal (Scanziani et al., 1998) slices. In some cases, this heterogeneity is dependent on the target cell type (Reyes et al., 1998). In addition, neurotrophic factors (Asztely et al., 2000; Davis and Murphey, 1994) and developmental changes control the differential formation of facilitating and depressing synapses (Pouzat and Hestrin, 1997; Reyes and Sakmann, 1999). In view of the present data and the essential role of Munc13-mediated vesicle priming for synaptic transmission (Augustin et al., 1999b), we propose that at least in some cases where functionally distinct facilitating and depressing synapses are observed in vivo, their differential equipment with Munc13 priming factors is causing the functional differences. Our data suggest a simple mechanism, i.e., switch from Munc13-1 to Munc13-2 in the presynaptic terminal or vice versa, by which a depressing or facilitating synaptic phenotype could be transformed into the respective other.

Features of Augmentation in Munc13-2-Dependent Synapses

In general, synaptic transmission is highly dependent on the recent history of presynaptic activity. During or following periods of stimulation, particularly at higher frequencies, most synapses show depression due to RRP depletion and, in many cases, due to a decrease of the vesicular release probability. However, forms of enhanced synaptic transmission following previous activation also exist. Depending on their time course and duration, these forms of synaptic enhancement are termed facilitation, augmentation, or potentiation (Zucker, 1989).

In the present study, a large and usually dominant population of depressing synapses was silenced by genetically abolishing the expression of Munc13-1. This manipulation unmasked a Munc13-2-dependent synapse population whose release properties at low-frequency stimulation are indistinguishable from wild-type, but in which one form of short-term plasticity, i.e., augmentation, dominates over other forms of plasticity. As observed in other systems, this augmentation develops within 300–1000 ms, is characterized by an up to 10-fold enhancement of synaptic transmission, decays with a time constant of approximately 8 s (Figure 4), and is strictly dependent on Ca^{2+} influx (Figure 7) (Zucker, 1989). Assuming that this type of Munc13-2-dependent synapse is not only present in our culture system but also relevant in situ, we used it as a model for augmentation and determined its characteristics.

Our functional analysis of Munc13-2-dependent synapses shows that augmentation is a consequence of both an increase of the RRP size and of the vesicular release probability (Figure 5). Most likely, the underlying molecular mechanism of augmentation involves a strong enhancement of Munc13-2-mediated priming activity in response to Ca^{2+}, leading to the observed increase of the RRP. The increase in vesicular release probability, on the other hand, can simply be explained by the facilitating action of elevated background Ca^{2+} concentrations on the release trigger. In contrast, previous studies in hippocampal cultures (Stevens and Wesseling, 1999) and other systems (Zucker, 1999) identified only increased vesicular release probabilities or pool refilling rates but no changes in the RRP size as causes for

activity-dependent changes in synaptic efficacy. The dramatic increase of the RRP in Munc13-2-dependent synapses (250%) is a unique type of synaptic enhancement in central neurons which likely was overseen in this preparation due to the small size of this synapse population. An interesting parallel is provided by chromaffin cells in which priming occurs in the presence of only very low Munc13-1 levels (Ashery et al., 2000) and the steady state RRP size is tightly regulated by Ca^{2+} in conjunction with PKC (Gillis et al., 1996; Smith et al., 1998).

The Role of Ca^{2+} in Augmentation and Its Possible Targets

In the present study, we demonstrate that both action potential trains at high-frequency (Figure 4) and K^+-induced depolarization (Figure 7) lead to strong augmentation in Munc13-2-dependent synapses, suggesting that influx of Ca^{2+} is the triggering signal. This interpretation is supported by the effects of EGTA-AM on augmentation in these cells (Figure 7D).

Our attempts to identify the target of this Ca^{2+} effect indicate that components of the Ca^{2+}-triggered release machinery are unlikely to be involved in the augmentation seen in Munc13-2-dependent cells. Likewise, enzymes involved in protein phosphorylation and dephosphorylation, and processes involving the regulation of vesicle mobility through modifications of cytoskeleton structure or function are unlikely to contribute to the Ca^{2+}-induced augmentation we observed (Figure 8A). However, given the pharmacological character of above experiments and the negative nature of the data, these conclusions must still be considered preliminary until more stringent genetic experiments provide more direct insights into the molecular basis of Munc13-2-dependent augmentation. According to our data, a more likely mechanism by which Ca^{2+} regulates Munc13-dependent short-term plasticity involves diacylglycerol-mediated activation of Munc13s. All Unc-13/Munc13 like proteins contain a conserved C_1 domain that binds diacylglycerol and its β-phorbol ester analogs. We show that β-phorbol ester-dependent potentiation of EPSCs mirrors the degree of train-induced augmentation (compare Figures 4 and 9), and that inhibition of PLC, which is itself a Ca^{2+}-dependent enzyme, prevents the induction of augmentation (Figure 8). In addition, experiments on mouse mutants in which the β-phorbol ester binding site of Munc13-1 was destroyed by homologous recombination (Munc13-1^{H567K}/Munc13-1^{H567K}) show that Munc13 C_1 domains play a key role in activity-dependent refilling of the RRP (Rhee et al., 2002). On the basis of these findings, the Ca^{2+} dependence of the enhanced pool refilling kinetics that underlies the augmentation in Munc13-2-dependent synapses may be the result of increased synaptic diacylglycerol levels following Ca^{2+}-dependent activation of PLCs. Similar to its role in PKC, the Munc13 C_1 domains would thus be ideally suited to respond to membrane-proximal and activity-induced increases of presynaptic Ca^{2+}/diacylglycerol concentrations with enhancement of Munc13 priming activity. The differences in short-term plasticity of distinct synapses formed by a single excitatory may therefore arise from the selective expression of Munc13 isoforms which themselves differ with respect to Ca^{2+}/diacylglycerol dependent priming activity.

Physiological Relevance of Depressing and Augmenting Synapses in a Single Axon

An increasing number of studies on basic synapse function appreciate the heterogeneity of synaptic function (Craig and Boudin, 2001). Synapses are not stereotypic translators of action potentials into neurotransmitter release, but rather vary with respect to size, postsynaptic sensitivity, equipment with modulatory signal transduction components, release probability, and dynamics of release over a wide range of presynaptic action potential frequencies.

We show here that the differential localization of Munc13s controls release dynamics of individual synapses. In vivo, such differences between synapses could be relevant in several different physiological contexts. First, different types of synapses formed by the same axon may allow a given nerve cell to transmit information of different quality in a target cell-dependent manner. In this scenario, different types of target cells (e.g., principal and interneurons within a brain region) would provide different targeting signals for Munc13 isoforms. Second, a balanced mix of facilitating and depressing synapses formed between two neurons by a single axon will broaden the bandwidth within which action potentials can be faithfully transduced into transmitter release. Finally, transforming depressing synapses into augmenting ones or vice versa by simply exchanging the Munc13 isoform may represent an important mechanism to induce lasting changes in synaptic efficacy, regardless of whether they follow developmental, learning, or even pathophysiological processes.

Experimental Procedures

Mutant Mouse Strains

Munc13-1 knockout mice were published previously (Augustin et al., 1999b). Munc13-2 knockouts were generated by homologous recombination in embryonic stem cells. In the targeting vector, a 6 kb genomic fragment containing multiple exons of the *Munc13-2* gene that are shared by the two Munc13-2 splice variants was replaced by a neomycine cassette. Recombinant stem cells were analyzed by Southern blotting of genomic DNA digested with EcoRI. Germline transmission was verified by Southern blotting and immunoblotting of brain extracts using an antibody against the C terminus of Munc13-2 (N. Brose et al., submitted). Munc13-1/2 double knockouts were produced by interbreeding of the respective single knockouts. These knockout mice are available for distribution.

Electrophysiology and Cell Culture

Microisland culture preparation was performed according to published procedures (Bekkers and Stevens, 1991; Augustin et al., 1999b). Data are expressed as mean ± SEM. Significance was tested using Student's t test or one-way ANOVA with the Bonferroni-Dunn procedure for multiple comparisons (Instat). Munc13-1 and Munc13-2 in-frame with EGFP were overexpressed in neurons using the Semliki Forest Virus system (GibcoBRL). pSFV1 constructs (GibcoBRL) encoding Munc13-1 or ubMunc13-2 in-frame with EGFP as well as virus production and infection protocols were published previously (Ashery et al., 2000; Betz et al., 2001). Drugs were dissolved in DMSO or as indicated by the supplier and were added to the external solution with at least 1000-fold dilution. Cypermethrin, calyculin A, cyclosporine, okadaic acid, latrunculin B, forskolin, U73343, U73122, and GÖ6983 were obtained from Calbiochem; EGTA-AM, PDBU, and Staurosporine from Sigma; kainate, MK-801, and GABA from Tocris.

Imaging Experiments

Hippocampal neurons were grown for 15–25 days on glass coverslips that served as the bottom glass of the perfusion chamber,

mounted on a stage of an inverted microscope (Olympus IX70) with an Olympus 40/1.35 or 60/1.4 NA oil objective. Fluorescence was excited at 488 ± 7.5 nm using a Xenon lamp with a grating monochromator (Polychrome II, TILL Photonics). Emitted fluorescence light was bandpass filtered (525–575 nm) and detected with a CCD camera (1300 × 1030 pixel resolution; Princeton Micromax 1300YHS). Images were taken every 7 s with a 500 ms exposure time. To identify and count active synapses, cells were stimulated and synchronously stained with 15 μM FM1-43 (Molecular Probes) in two experiments per sample. In the first run, cells were stimulated by action potential induction (15 Hz, 10 s), in the second run by K^+-induced depolarization (15 s; with modified external medium: 65 mM K^+, 104.4 mM Na^+). To release the endocytosed dye, neurons were stimulated again 180 s after staining by induction of action potentials (15 s, 20 Hz) or K^+-mediated depolarization (20 s, 65 mM). All imaging experiments were performed at 30°C. We recorded the images using Axon Imaging Workbench 2.2 (Axon Instruments) and analyzed them with TILLvisION 3.3 (TILL Photonics). For each series of images, we calculated the amount of specific destaining upon stimulation of the neuron for each pixel. The amount of specific destaining (due to evoked exocytosis of stained vesicle content) was calculated from the fluorescence intensities in three images, which were recorded at 21 s time intervals: the first and the second image were recorded before stimulation/unloading of the cell, the third after stimulation/unloading. The unloading procedure was performed immediately following the acquisition of the second image. Unspecific destaining (ΔI_u) due to bleaching and passive diffusion of FM1-43 in the time interval between two stimuli was quantified by subtracting the second image from the first. The sum of specific and unspecific destaining (ΔI_t) was determined by subtracting the third image from the second one. The amount of specific destaining (ΔI_s) was then calculated by subtracting ΔI_u from ΔI_t. To identify all synapses independently of their exocytotic activity, the cultures from the FM1-43 experiments were fixed as described (Betz et al., 1998) and stained with a primary monoclonal antibody directed against Synaptophysin (Synaptic Systems) followed by an Alexa-488-labeled secondary antibody (Molecular Probes). Fluorescence images were taken from the same subcellular regions that were observed during FM1-43 recordings.

Acknowledgments

We thank F. Benseler, T. Hellmann, I. Herfort, I. Thanhäuser. S. Wenger, and A. Zeuch for excellent technical assistance, and the staff of the animal facility at the Max-Planck-Institute for Experimental Medicine for blastocyst injections and maintenance of mouse colonies. We are grateful to E. Neher, T.C. Südhof, and J. Rettig for support and advice. This study was supported by grants from the Deutsche Forschungsgemeinschaft (SFB406/A1 to N.B.; Ro1296/5-1 to C.R.) and by Heisenberg Fellowships from the Deutsche Forschungsgemeinschaft to N.B. and C.R.

Received November 7, 2000; revised December 7, 2001.

References

Aravamudan, B., Fergestad, T., Davis, W.S., Rodesch, C.K., and Broadie, K. (1999). Drosophila UNC-13 is essential for synaptic transmission. Nat. Neurosci. *2*, 965–971.

Ashery, U., Varoqueaux, F., Voets, T., Betz, A., Thakur, P., Koch, H., Neher, E., Brose, N., and Rettig, J. (2000). Munc13-1 acts as a priming factor for large dense-core vesicles in bovin chromaffin cells. EMBO J. *19*, 3586–3596.

Asztely, F., Kokaia, M., Olofsdotter, K., Örtegren, U., and Lindvall, O. (2000). Afferent-specific modulation of short-term synaptic plasticity by neurotrophins in dentate gyrus. Eur. J. Neurosci. *12*, 662–669.

Augustin, I., Betz, A., Herrmann, C., Jo, T., and Brose, N. (1999a). Differential expression of two novel Munc13 proteins in rat brain. Biochem. J. *337*, 363–371.

Augustin, I., Rosenmund, C., Südhof, T.C., and Brose, N. (1999b). Munc13-1 is essential for fusion competence of glutamatergic synaptic vesicles. Nature *400*, 457–461.

Augustin, I., Korte, S., Rickmann, M., Kretzschmar, H.A., Südhof, T.C., Herms, J.W., and Brose, N. (2001). The cerebellum-specific Munc13 isoform Munc13-3 regulates cerebellar synaptic transmission and motor learning in mice. J. Neurosci. *21*, 10–17.

Bekkers, J.M., and Stevens, C.F. (1991). Excitatory and inhibitory autaptic currents in isolated hippocampal neurons maintained in cell culture. Proc. Natl. Acad. Sci. USA *88*, 7834–7838.

Betz, A., Ashery, U., Rickmann, M., Augustin, I., Neher, E., Südhof, T.C., Rettig, J., and Brose, N. (1998). Munc13-1 is a presynaptic phorbol ester receptor that enhances neurotransmitter release. Neuron *21*, 123–136.

Betz, A., Thakur, P., Junge, H.J., Ashery, U., Rhee, J.-S., Scheuss, V., Rosenmund, C., Rettig, J., and Brose, N. (2001). Functional interaction of the active zone proteins Munc 13-1 and RIM1 in synaptic vesicle priming. Neuron *30*, 183–196.

Cochilla, A.J., Angleson, J.K., and Betz, W.J. (1999). Monitoring secretory membrane with FM1–43 fluorescence. Annu. Rev. Neurosci. *22*, 1–10.

Craig, A.M., and Boudin, H. (2001). Molecular heterogeneity of central synapses: afferent and target regulation. Nat. Neurosci. *4*, 569–578.

Davis, G.W., and Murphey, R.K. (1994). Long-term regulation of short-term transmitter release properties: retrograde signaling and synaptic development. Trends Neurosci. *17*, 9–13.

Gillis, K.D., Mößner, R., and Neher, E. (1996). Protein kinase C enhances exocytosis from chromaffin cells by increasing the size of the readily releasable pool of secretory granules. Neuron *16*, 1209–1220.

Harris, K.M., and Stevens, J.K. (1989). Dendritic spines of CA 1 pyramidal cells in the rat hippocampus: serial electron microscopy with reference to their biophysical characteristics. J. Neurosci. *9*, 2982–2997.

Helmchen, F., Imoto, K., and Sakmann, B. (1996). Ca^{2+} buffering and action potential-evoked Ca^{2+} signaling in dendrites of pyramidal neurons. Biophys. J. *70*, 1069–1081.

Hessler, N.A., Shirke, A.M., and Malinow, R. (1993). The probability of transmitter release at a mammalian central synapse. Nature *366*, 569–572.

Ma, L., Zablow, L., Kandel, E.R., and Siegelbaum, S.A. (1999). Cyclic AMP induces functional presynaptic boutons in hippocampal CA3–CA1 neuronal cultures. Nat. Neurosci. *2*, 24–30.

Malgaroli, A. (1999). Silent synapses: I can't hear you! Could you please speak aloud? Nat. Neurosci. *2*, 3–5.

Murthy, V.N., Sejnowski, T.J., and Stevens, C.F. (1997). Heterogeneous release properties of visualized individual hippocampal synapses. Neuron *18*, 599–612.

Pouzat, C., and Hestrin, S. (1997). Developmental regulation of basket/stellate cell→Purkinje cell synapses in the cerebellum. J. Neurosci. *17*, 9104–9112.

Reyes, A., and Sakmann, B. (1999). Developmental switch in the short-term modification of unitary EPSPs evoked in layer 2/3 and layer 5 pyramidal neurons of rat neocortex. J. Neurosci. *19*, 3827–3835.

Reyes, A., Lujan, R., Rozov, A., Burnashev, N., Somogyi, P., and Sakmann, B. (1998). Target-cell-specific facilitation and depression in neocortical circuits. Nat. Neurosci. *1*, 279–285.

Richmond, J.E., Davis, W.S., and Jorgensen, E.M. (1999). UNC-13 is required for synaptic vesicle fusion in C. elegans. Nat. Neurosci. *2*, 959–964.

Rhee, J.S., Betz, A., Pyott, S., Reim, K., Varoqueaux, F., Augustin, I., Hesse, D. Südhof, T.C., Takahashi, M., Rosenmund, C., and Brose, N. (2002). β Phorbol ester- and diacylglycerol-induced augmentation of transmitter release is mediated by Munc13s and not by PKCs. Cell *108*, 121–134.

Rosenmund, C., and Stevens, C.F. (1996). Definition of the readily releasable pool of vesicles at hippocampal synapses. Neuron *16*, 1197–1207.

Rosenmund, C., Clements, J.D., and Westbrook, G.L. (1993). Nonuniform probability of glutamate release at a hippocampal synapse. Science *262*, 754–757.

Scanziani, M., Gähwiler, B.H., and Charpak, S. (1998). Target cell-specific modulation of transmitter release at terminals from a single axon. Proc. Natl. Acad. Sci. USA *95*, 12004–12009.

Schikorski, T., and Stevens, C.F. (1997). Quantitative ultrastructural analysis of hippocampal excitatory synapses. J. Neurosci. *17*, 5858–5867.

Smith, C., Moser, T., Xu, T., and Neher, E. (1998). Cytosolic Ca2+ acts by two separate pathways to modulate the supply of release-competent vesicles in chromaffin cells. Neuron *20*, 1243–1253.

Stevens, C.F., and Sullivan, J.M. (1998). Regulation of the readily releasable vesicle pool by protein kinase C. Neuron *21*, 885–893.

Stevens, C.F., and Wesseling, J.F. (1999). Augmentation is a potentiation of the exocytotic process. Neuron *22*, 139–146.

Thomson, A.M. (1997). Activity-dependent properties of synaptic transmission at two classes of connections made by rat neocortical pyramidal axons *in vitro*. J. Physiol. (Lond.) *502*, 131–147.

Wadiche, J.I., and Jahr, C.E. (2001). Multivesicular release at climbing fiber-purkinje cell synapses. Neuron *32*, 301–313.

Walmsley, B., Alvarez, F.J., and Fyffe, R.E. (1998). Diversity of structure and function at mammalian central synapses. Trends Neurosci. *21*, 81–88.

Wang, L.Y., and Kaczmarek, L.K. (1998). High-frequency firing helps replenish the readily releasable pool of synaptic vesicles. Nature *394*, 384–388.

Zucker, R.S. (1989). Short-term synaptic plasticity. Annu. Rev. Neurosci. *12*, 13–31.

Zucker, R.S. (1999). Calcium- and activity-dependent synaptic plasticity. Curr. Opin. Neurobiol. *9*, 305–313.